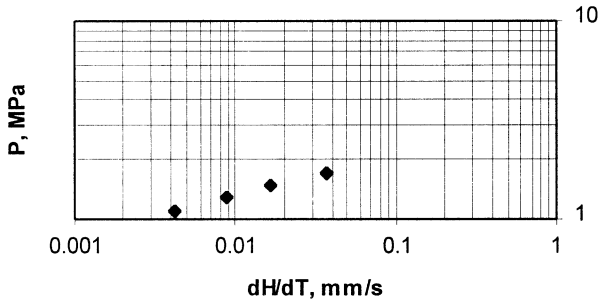

Fig. 6—Plot of forming pressure, *P*, against average rate of forming, *dH*/*dt*.

cavitation is likely to be delayed if superplastic forming is done at temperatures beyond 950 °C.

Cone heights as a function of forming pressure after 1 hour of forming are shown in Figure 5. With increase in forming pressure for stipulated forming time, there is a increase in the cone height. By knowing the height of the cone and time it takes to attain the height, it is possible to calculate average rate of forming (*dH*/*dt*).

For $H < R$ (where H is the cone height and R is the radius of the die), the situation is similar to free bulge forming. Under this condition, we could apply curved bubble thin film solution, and flow stress of the forming material can then be expressed as $\sigma_c = (PR)/(2T)$, where P is the forming pressure, T is the thickness of the sheet, and σ_c is the flow stress of the material that is being formed. The slope of the graph of *dH*/*dt vs P* plotted on a logarithmic scale is similar to the strain rate sensitivity (m) measured by performing tensile tests.[6] For $H < R$, the slope of the *dH*/*dt vs P* should provide an approximate estimate of m or measure of superplasticity. Figure 6 is a plot of *dH*/*dt vs* forming pressure *P*. The slope of the plot corresponds to a strain rate sensitivity of 0.2, which is close to the strain rate sensitivity value reported by Pulino-Sagaradi *et al.* for duplex stainless steel at 950 °C.[7]

In conclusion, preliminary attempts were made to superplastically form duplex stainless steel. Because of the limitation posed by the SPF machine, maximum forming temperature could not exceed 950 °C. Pressures as high as 1.7 MPa had to be maintained during the superplastic forming operation. Based on the present study, it appears that use of higher forming temperature will not only require lower forming pressure but also make it easier to use back pressure to suppress cavitation, thereby increasing the extent of forming.

REFERENCES

1. J.O. Nilsson: *Mater. Sci. Technol.* 1992, vol. 8, pp. 685-700.
2. H.W. Hayden, R.C. Gibson, H.F. Merrik, and J. Brophy: *Trans. ASM*, 1967, vol. 60, pp. 3-14.
3. J. Pilling and N. Ridley: *Acta Metall.*, 1986, vol. 34, pp. 669-79.
4. Y. Maehara: *Metall. Trans. A*, 1991, vol. 22A, pp. 1083-91.
5. M. Sagaradi, D. Pulino-Sagaradi, and R.E. Medrano: *Acta Metall.*, 1998, vol. 46, pp. 3857-62.
6. R. Fotedar, R. Kishore, B.P. Kashyap, and S. Banerjee: *Mater. Sci. Forum*, 1997, vols. 243–245, pp. 663-68.
7. D. Pulino-Sagaradi, A.M.M. Nazar, J.J. Ammann, and R.E. Medrano: *Acta Metall.*, 1997, vol. 45, pp. 4663-66.

Chemical Synthesis and Characterization of Low Thermal Expansion–High Conductivity Cu-Mo and Ag-Mo Composites

J. STOLK and A. MANTHIRAM

Heat dissipation and thermal expansion mismatch are extremely important issues in many electrical and electronics applications, and the materials used for thermal management in such applications have attracted a great deal of attention in recent years. The move in the microelectronics industry toward higher circuit board chip densities and packageless chip designs such as flip chips has prompted the need for improved thermal management materials. If heat extraction and thermal expansion are not properly addressed, thermal mismatch among the materials in electronic assemblies may lead to high interfacial shear strains and premature component failure.

Core constraining materials and heat sinks are sometimes used to improve the reliability of modern printed wiring boards that incorporate dense packing of packageless flip chips and leadless chip carriers. Ideally, core constraining and heat sink materials should have low thermal expansion coefficients to reduce thermal mismatch strains and high thermal conductivity to assist in the extraction of heat. A variety of low thermal expansion, high conductivity composites are currently available,[1–6] but many of these composites have high manufacturing costs or anisotropic properties.

Nanocrystalline powder metallurgy alloys with intimately mixed components may offer the desired thermal and electrical properties at manufacturing costs lower than some of the materials currently in use. The present study aims at the production of nanocrystalline copper-molybdenum and silver-molybdenum powders using solution-based synthesis techniques, formation of fine-grained alloys by heat treatment, and characterization of the resulting products.

Fine-grained Cu-Mo and Ag-Mo alloys were prepared by reducing nanocrystalline oxide precursors in a H_2 atmosphere at an elevated temperature. The copper molybdate precursor was prepared by mixing aqueous solutions of $Cu(CH_3COO)_2 \cdot H_2O$ (copper acetate) and $(NH_4)_6Mo_7O_{24} \cdot 2H_2O$ (ammonium paramolybdate), and the silver molybdate precursor was prepared by mixing aqueous $AgNO_3$ (silver nitrate) and $(NH_4)_6Mo_7O_{24} \cdot 2H_2O$ (ammonium paramolybdate) solutions. The compositions of the products were controlled by adjusting the relative amounts of solutions and the pH during the reaction, with higher pH giving higher molybdenum content. The copper molybdate precipitate that formed during the reaction was greenish, and the silver molybdate precipitate was pale yellow. The precipitates were washed repeatedly with water to remove any ions that did not participate in the reaction.

The as-prepared Cu-Mo-O and Ag-Mo-O powders were

J. STOLK, Visiting Assistant Professor, formerly at Texas Materials Institute, The University of Texas at Austin, is with the Chemical Engineering Department, Bucknell University, Lewisburg, PA 17837. A. MANTHIRAM, Professor, is with the Texas Materials Institute, The University of Texas at Austin, Austin, TX 78712.

Manuscript submitted March 28, 2000.

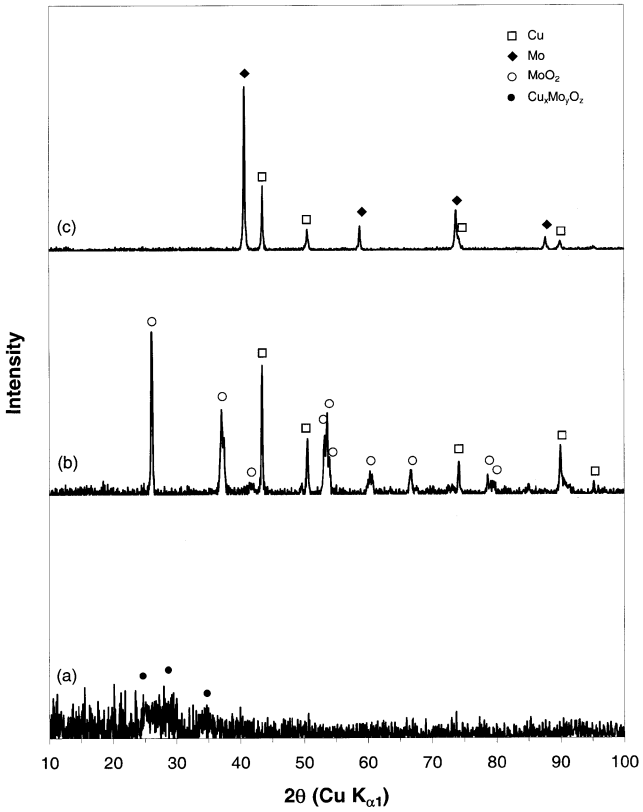

Fig. 1—XRD patterns of sample A (52.5 wt pct Cu−47.5 wt pct Mo): (*a*) as-prepared copper molybdate precursor and after annealing in H_2 at (*b*) 500 °C and (*c*) 1050 °C.

initially heated in H_2 to reduce the compounds to metallic Cu and Mo or Ag and Mo. After annealing, the powders were compacted in a hydraulic press and sintered at 800 °C to 1050 °C in a H_2 atmosphere. X-ray diffraction (XRD), energy dispersive X-ray spectroscopy (EDS), and scanning electron microscopy (SEM) were used to characterize the products. Thermal expansion behavior was evaluated at 20 °C to 300 °C with a thermomechanical analyzer. Electrical conductivity was measured by a four-probe technique, and thermal conductivity was estimated using the Wiedemann–Franz law.

Sample identifications and compositions as determined by EDS of several as-prepared Cu-Mo and Ag-Mo powders are shown in Table I. The X-ray diffraction patterns of the as-prepared and heat-treated sample A (52.5 wt pct Cu-47.5 wt pct Mo) are shown in Figure 1. In the as-prepared condition, relative intensity is low and no distinct X-ray diffraction reflections are present, indicating extremely small grain size in the as-prepared powder. The broad reflections that are observed in Figure 1(a) for the as-prepared powder correspond to the major peaks of several different $Cu_xMo_yO_z$ copper molybdate compounds such as $CuMoO_4$, $Cu_3Mo_2O_9$, and Cu_2MoO_5. After annealing at 500 °C in H_2, reflections corresponding to metallic Cu and molybdenum dioxide (MoO_2) are evident, indicating partial reduction of the Cu_x-Mo_yO_z powder. Above 800 °C, only metallic (Cu) and (Mo) diffraction peaks are present, indicating complete reduction of the oxide precursor.

The as-prepared powders are approximately 5 to 10 nm in size and tend to agglomerate into larger powder clusters of approximately 50 nm in size, as shown in Figure 2(a) for as-prepared Ag-Mo-O. After annealing at 500 °C for 2 hours in H_2, the Cu particle size increases to approximately 500 nm, and the particle size of the Mo-rich phase increases to approximately 150 nm, as shown in Figure 2(b). Sintering Cu-Mo at 1050 °C in H_2 for 1 hour yields a uniform distribution of Cu and Mo grains and an average grain size of approximately 0.5 μm, as shown in Figure 2(c). Phases in the heat-treated alloys were identified by spot EDS analysis.

Table I shows the average coefficient of thermal expansion (CTE) in the temperature range of 25 °C to 100 °C, electrical conductivity, estimated thermal conductivity, and hardness of the Cu-Mo and Ag-Mo composites. Thermal expansion of the Cu-Mo and Ag-Mo is linear from 25 °C to 300 °C and close to Cu-Mo and Ag-Mo values predicted by a rule-of-mixtures, or isostress, model. Electrical conductivity decreases with increasing molybdenum content. Hardness values of sintered Cu-Mo and Ag-Mo are high due to the small grain size, and hardness increases with molybdenum content.

In summary, nanocrystalline Cu-Mo-O and Ag-Mo-O were prepared using simple chemical precursor techniques. Homogeneous, two-phase alloys of Cu-Mo and Ag-Mo are formed upon pressureless sintering of powders in a H_2 atmosphere at 800 °C to 1050 °C. The CTE and electrical conductivity of the Cu-Mo and Ag-Mo alloys decrease with increasing molybdenum content, and specific values of CTE and conductivity are easily obtainable by this procedure. The thermal and electrical properties of the Cu-Mo and Ag-Mo alloys prepared by this method are comparable to existing low CTE-high conductivity materials, and the small grain size and isotropic properties of the fine-grained alloys offer distinct mechanical property advantages over some of the materials currently in use.

Table I. Sample Identification, Composition, and Properties of Sintered Cu-Mo and Ag-Mo

Sample	Composition, Wt Pct	Average CTE, $°C^{-1}$	Electrical Conductivity, S/cm	Estimated Thermal Conductivity, W/m · K	Hardness, HV_{5kg}
A	52.5Cu - 47.5Mo	11.9×10^{-6}	3.2×10^5	240	200
B	44.6Cu - 55.4Mo	9.98×10^{-6}	2.9×10^5	210	252
C	36.1Cu - 63.9Mo	8.65×10^{-6}	2.9×10^5	210	257
D	44.0Ag - 56.0Mo	10.2×10^{-6}	2.7×10^5	200	239
E	38.1Ag - 61.9Mo	9.48×10^{-6}	2.3×10^5	170	251

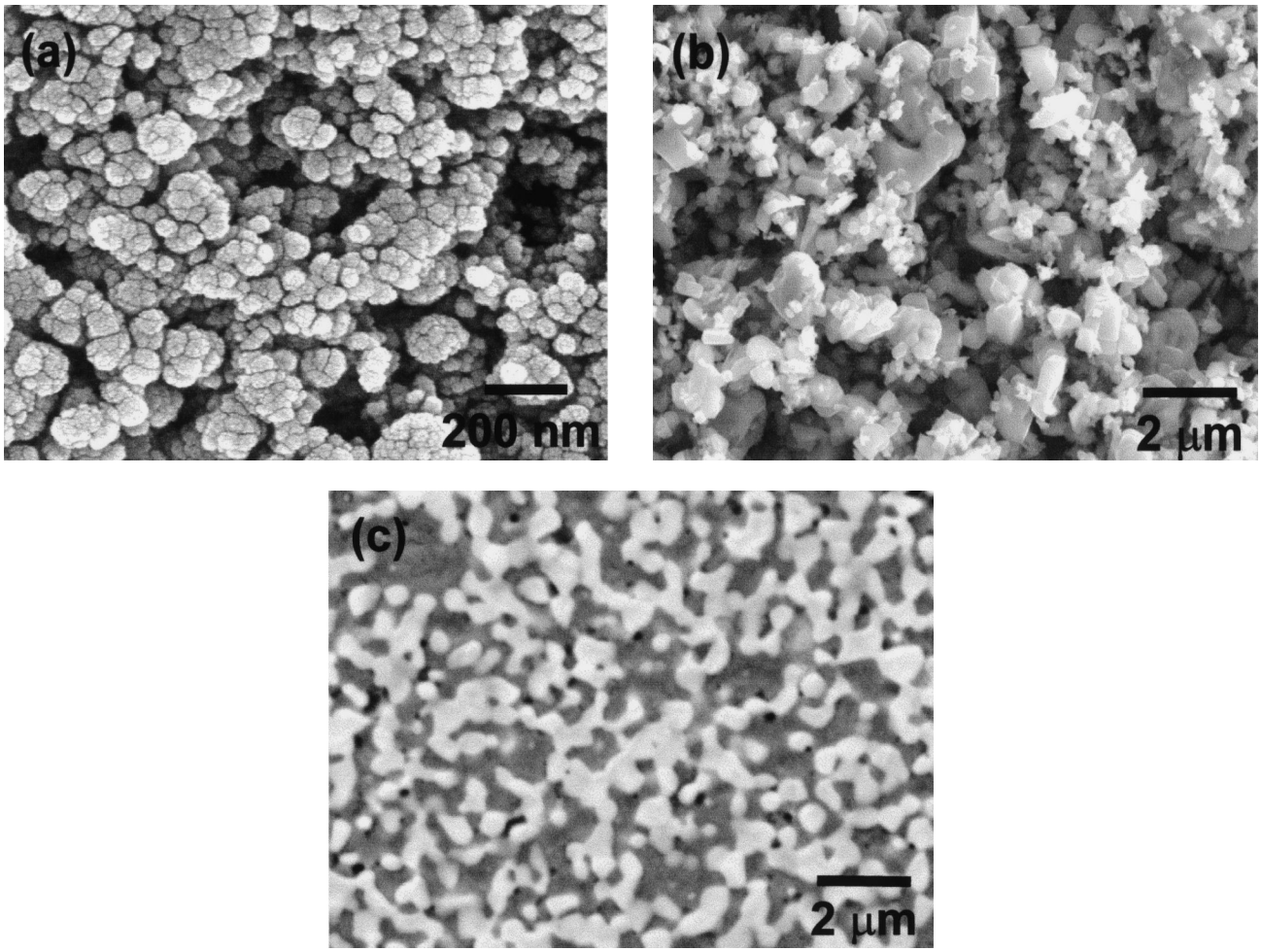

Fig. 2—SEM images of Ag-Mo and Cu-Mo: (*a*) sample D (44 wt pct Ag-56 wt pct Mo) as-prepared powder agglomerates, (*b*) sample A (52.5 wt pct Cu-47.5 wt pct Mo) after annealing in H_2 at 500 °C for 2 h, and (*c*) sample A (52.5 wt pct Cu-47.5 wt pct Mo) after sintering in H_2 at 1050 °C (backscattered electron image). In Fig. 2(b), the large, darker particles are Cu and small, and the lighter particles are MoO_2. In Fig. 2(c), light grains are (Mo), dark gray grains are (Cu), and black spots are pores.

REFERENCES

1. W.R. Johannes and W. Johnson: *Int. J. Microcircuits Elec. Packaging*, 1994, vol. 17 (2), pp. 135-42.
2. D.E. Jech and J.L. Sepulveda: *Int. Symp. on Microelectronics*, Las Vegas, NV, 1997, SPIE Proc. Series 3235, SPIE, pp. 90-96.
3. P. Yih and D.D.L. Chung: J. Mater. Sci., 1997, vol. 32, pp. 2873-82.
4. C. Zweben: *JOM*, 1992, vol. 44(7), pp. 15-22.
5. R. Kumar, J.J. Stiglich, T.S. Sudarshan, and C.C. Yu: *Mater. Manufacturing Processes*, 1996, vol. 11, pp. 1029-41.
6. S. Yamagata, M. Imamura, Y. Hirose, Y. Abe, Y. Takano, and A. Fukui: *Int. Symp. on Microelectronics*, San Diego, CA, 1998, SPIE Proc. Series 3582, SPIE, pp. 675-80.